Journal of Chemical and Petroleum Engineering (JChPE)

Print ISSN: 2423-673X Online ISSN: 2423-6721

Quantifying Uncertainty of Green Inhibition Efficiency of Luffa Cylindrica Leaf Extract on Mild Steel in Acidic Medium

Akeem Olatunde Arinkoola*, Eunice Folasayo Oyelade, Mariam Omowumi Alesinladu, Azeez Gbolahan Akinyemi, Solomon Oluyemi Alagbe, Oladipupo Olaosebikan Ogunleye

1. Department of Chemical Engineering, Ladoke Akintola University of Technology, Ogbomoso, Nigeria. Department of Chemical and Petroleum Engineering, First Technical University, Ibadan, Nigeria. E-mail: aoarinkoola@lautech.edu.ng
2. Department of Chemical Engineering, Ladoke Akintola University of Technology, Ogbomoso, Nigeria. E-mail: efoyelade@student.lautech.edu.ng
3. Department of Chemical Engineering, Ladoke Akintola University of Technology, Ogbomoso, Nigeria. E-mail: mariamomowumi003@gmail.com
4. Department of Chemical Engineering, Ladoke Akintola University of Technology, Ogbomoso, Nigeria. E-mail: azeezakinyemi61@gmail.com
5. Department of Chemical Engineering, Ladoke Akintola University of Technology, Ogbomoso, Nigeria. E-mail: soalagbe@lautech.edu.ng
6. Department of Chemical Engineering, Ladoke Akintola University of Technology, Ogbomoso, Nigeria. E-mail: ooogunleye@lautech.edu.ng

ARTICLE INFO

Article History:
Received: 28 December 2023
Revised: 17 February 2024
Accepted: 19 February 2024

Article type: Research

Keywords:
Green Inhibitor,
Inhibition Efficiency,
Luffa Cylindrical,
Monte Carlo Simulation,
Uncertainty Analysis

ABSTRACT

Green corrosion inhibitors, such as Luffa Cylindrica leaf extract, have demonstrated outstanding inhibitory efficiency on mild steel in acidic environments. However, their effective design and optimization for field applications are limited and time-consuming owing to the associated uncertainties. Quantifying these uncertainties remains a challenge due to the requirement of many model realisations to capture and represent the true distribution of uncertainty. This study built a Response Surface Model (RSM) approximation of corrosion inhibition efficiency (IE) for effective optimization and uncertainty propagation. To quantify the uncertainties, we explored two stochastic methods: Monte Carlo Simulation (MCS) and Markowitz classical theory with the Genetic Algorithm (GA). The two approaches differ in propagation, sampling, and the number of realizations. MCS uses the approximation RSM with 10,000 randomly generated realizations, whereas the Markowitz technique uses the mean-variance objective function with just 100 realizations. Markowitz's classical theory revealed a 50 and 99.9% chance that the IE of Luffa Cylindrica leaf extract is 79.7 and 76.5%, respectively while MCS indicates at least 10 and 90% probabilities that the IE of Luffa Cylindrica leaf extract is 85.16 and 74.14%, respectively. When compared to the 88.4% efficiency previously reported for the same extract, the two techniques indicate less than 10% chances for IE. As a result, for the actual implementation of green inhibitors, their assessment must include uncertainty analysis.

* Corresponding Authors: A.O. Arinkoola (E-mail address: aoarinkoola@lautech.edu.ng)

Journal of Chemical and Petroleum Engineering, 2024, 58(1): 189- 207.
Publisher: University of Tehran, College of Engineering DOI: 10.22059/jchpe.2024.370271.1473

Introduction

When a metal is exposed to its environment, electrochemical processes occur, which leads to corrosion. Metal corrosion is a serious issue that costs a lot of money and impacts negatively every production sector. Every year, billions of dollars are spent internationally to fight corrosion and prevent disasters [1]. As a result, corrosion prevention is a vast study topic with many distinct techniques [2]. Corrosion can be minimized through careful design, appropriate material selection, electrochemical (anodic and cathodic) protection, protective coatings, and the use of corrosion inhibitors [3]. The application of a corrosion inhibitor is frequently regarded as the most viable and time-efficient of these options. Synthetic inhibitors are organics with structures that are predominantly composed of nitrogen, sulfur, or oxygen atoms [4]. They are very efficient yet, costly and non-biodegradable [5, 6]. Many plant extracts are utilized, including Mangifera indica (mango) seed, bark, and leaf extract [7], orange peel extract [8], leaf and stem extract of *Sida acuta* [9], Pawpaw leaf extract, groundnut leave extract, kola leaf extract, [10,11], neem leaf extract [12,13], *Psidium Guajava* Leaf Extract [14], *Luffa Cylindrica* leaf extract [15]. The popularity of these extracts was ascribed to their eco-friendliness, non-toxic nature, environmental friendliness, and accessibility.

Various plant extract evaluation studies are currently restricted to the laboratory, and the thorough approaches for connecting field extract performance with a controlled corrosion experiments are still insufficient for many reasons [16]. A variety of factors can aid metal corrosion, including their reactivity, the presence of contaminants, the pH and temperature of the solution, and industrial practices such as acidizing, acid cleaning, pickling, descaling, and so on. Understanding how these uncertainties impact the anticipated corrosion rate in a controlled setting is a good starting point for building this correlation [17]. The analytical methods used to measure corrosion inhibitor effectiveness are based on electrochemical approaches and weight loss from immersion tests [1]. In the electrochemical operations, the Tafel extrapolation methods, electrochemical impedance spectroscopy (EIS), linear polarization resistance (LPR), or a combination of these techniques are frequently utilized [3]. Using these approaches, Tafel's experiment has been linked to the subsequent systemic and stochastic errors [2, 3]. The Tafel approach takes into account the relationship between current density and overvoltage. Eq. 1 is used to compute the corrosion rate for mild steel using the linear polarization method (LPR).

$$CR = 0.503 \frac{\beta_a \beta_c}{(\beta_a + \beta_c)} * \frac{1}{R_p} \tag{1}$$

Thus, the relative deviation of CR calculation due to component variables can be expressed by Eq. 2 [17,18].

$$\begin{aligned} \frac{\partial CR}{CR} &= \left[\frac{\partial (CR)}{\partial T}\right]\frac{\partial T}{CR} + 2\left[\frac{\partial (CR)}{\partial E}\right]\frac{\partial E}{CR} + 2\left[\frac{\partial (CR)}{\partial I_{app}}\right]\frac{\partial I_{app}}{\partial CR} + 2\left[\frac{\partial (CR)}{\partial a}\right]\frac{\partial a}{CR} \\ \frac{\partial CR}{CR} &= \left[\frac{m_1}{\beta_a} + \frac{m_2}{\beta_c}\right]\partial T - \frac{2}{E}\partial E + \frac{2}{I_{app}}\partial I_{app} - \partial_a \end{aligned} \tag{2}$$

Thus, the total uncertainty factors in LPR corrosion computation are caused by instrumentation (potential, applied current, working electrode surface area) and Tafel slope, (β)[2]. Previous research has shown that during corrosion analysis, to assume linearity while determining the Tafel slopes can generate errors of 34-50% [19, 20]. Similarly, the assumption that the corrosion process does not vary across a potential range of several hundred millivolts

to establish the uniform rate of corrosion may add some degree of inaccuracy into the study [21].

In the immersion test, the CR and IE are generally computed using Eq. 3 and 4 [6,15, 22]. The values of these model inputs should ideally correspond to those of the actual system. However, because the inputs are prone to experimental variability and measurement error, there is a mismatch between what is measured or reported as the input to the physical system and its real value. The computational model's capacity for model prediction would therefore be constrained since the inputs used by the model and the real system are different [23]. To compute the corrosion rate for test runs in line with ASTM G31 Standard Practice for Laboratory Immersion, Freeman [24] has examined how statistical errors in the variables on the right side of Eq. 3 statistically propagate through to CR by Eq. 5.

$$CR = \frac{\alpha(m_0 - m_f + m_c)}{\rho A(t_f - t_0)} \tag{3}$$

$$IE = \frac{(CR_0 - CR_f)}{CR_0} * 100 \tag{4}$$

$$V_{unc}(R) \approx \left[\frac{\partial R}{\partial m_f}\right]^2 \sigma_{mf}^2 + \left[\frac{\partial R}{\partial m_c}\right] \sigma_{mc}^2{}^2 + \left[\frac{\partial R}{\partial m_i}\right]^2 \sigma_{mi}^2 + \left[\frac{\partial R}{\partial t_f}\right]^2 \sigma_{tf}^2 + \left[\frac{\partial R}{\partial t_i}\right]^2 \sigma_{ti}^2 + \left[\frac{\partial R}{\partial A}\right]^2 \sigma_A^2 \tag{5}$$

where m_o and m_f are the initial and final masses in g, t_o and t_f are the initial and final times in h, respectively, A is the surface area cm^2, ρ is the density g/cm^3, and α is a constant (87 600 mm cm^{-1} h $year^{-1}$). The term m_c (g) indicates the extra loss of base metal caused by eliminating the corrosion products.

Vunc is the variance of the uncertainty, σ*m* represents the standard deviation in the measurement of mass, σ*t* represents the standard deviation in the measurement of time, and σ*A* represents the standard deviation in the measurement of area. The subscripts "*i*", "*f*" and "*c*" stand for initial, final, and cleaning, respectively.

Another source of uncertainty in IE is a lack of thorough understanding of the corrosion process and/or contributing variables. When evaluating different green inhibitors, many researchers frequently look at the effects of temperature, concentrations (of medium and inhibitors), and immersion time [22, 25]. The result is highly unclear since a number of other elements that affect the corrosion process are ignored. The use of surrogate models in the optimization research is another cause of error. Empirical correlations are often applied in engineering to reduce computing costs and make project choices easier [26]. Response surface models, for example, have found use in corrosion research for sensitivity analysis, chemical synthesis, and optimization [1, 27].

Previous attempts in green corrosion inhibition studies seldom took uncertainty into account when assessing various plant extracts as anti-corrosion in metals exposed to acid and salt media. As a result, assessing the IE of *Luffa Cylindrica* leaf extract uncertainty is considered in this work. Quantifying uncertainties remains a challenge due to the requirement of many model realisations to capture and represent the true distribution of uncertainty. This study built a Response Surface Model (RSM) approximation of corrosion inhibition efficiency (IE) for effective optimization and uncertainty propagation and quantify the uncertainties, by exploring two stochastic methods: Monte Carlo Simulation (MCS) and Markowitz classical theory with the Genetic Algorithm (GA). The work flow of the two methods is depict in Fig. 1.

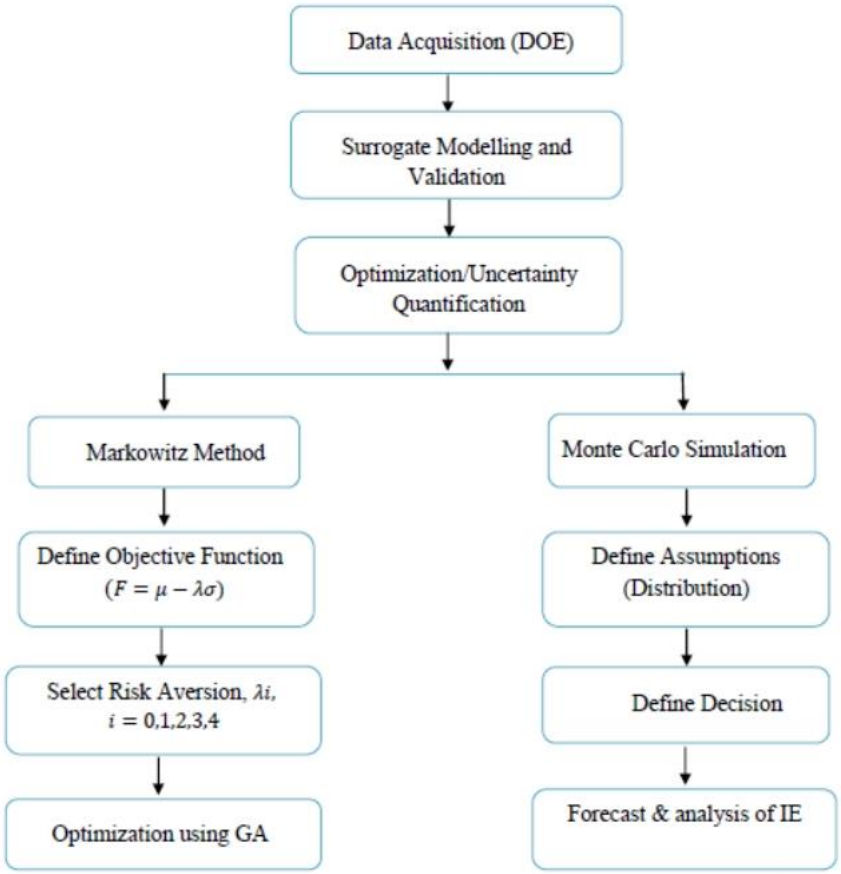

Fig. 1. Workflow of the proposed Markowitz and Monte Carlo Simulation

Material and Methods

Batch Corrosion Study

The *Luffa Cylindrica* leaf extract was obtained by the soxhlet extraction method using analytical grade ethanol as solvent. To identify the individual compounds in the extracts, the Gas Chromatograph-Mass Spectrometry (GC-MS) technique was used. FT-IR spectroscopy was also used for the qualitative analysis to identify the functional groups present in the extract. The detailed result from the characterization of the extract is available in [15]. The extract was tested for corrosion inhibition of mild steel coupons (22 mm x 36 mm x 3 mm) in 0.5 M HCl solution using the weight loss method [6]. The preliminary investigation was carried out at room temperature (30 ± 0.5^0C) for various concentrations of L*uffa cyclindrica* leaf extract (0.2-1.2g/L) for 24 days. A batch corrosion study was thereafter carried out at different concentrations (0.5-1.0 g/L) of *Luffa cyclindrica* extract placed in a thermostat water bath shaker (Model: SHAC1) to determine the effect of temperatures (30 - 60 °C) and immersion time (4-12 h).

The initial and final weight of the mild steels was measured using a precision balance (WJEUIP, Model JA 6003B) of 0.001g sensitivity. The measurements were replicated three times to minimize the experimental error.

The weight loss and the IE of the *Luffa Cylindrical* extract were calculated using Eq. 6 and 7, respectively. the result in terms of corrosion rate is as presented as shown in Table 1.

$$W = W_i - W_f \quad (6)$$

$$IE = 100\left(\frac{W_o - W_1}{W_o}\right)\% \quad (7)$$

where W = weight loss, W_i = initial weight, W_f = final weight. Where, W_o and W_1 are the weight loss of mild steel in the absence and presence of inhibitor in HCl medium at the same temperature respectively.

Table 1. Weight loss recorded at ambient conditions for different concentrations and immersion time

Inh. Conc	Immersion time (h)						
(g/l)	24	48	72	96	120	144	168
0	1.1100±0.01	1.1200±0.07	1.1400±0.01	1.1800±0.01	1.2000±0.02	1.2400±0.00	1.4454±0.00
0.2	0.5994±0.08	0.5227±0.06	0.4594±0.01	0.4153±0.03	0.3956±0.01	0.3793±0.01	0.4425±0.01
0.4	0.4956±0.05	0.4322±0.10	0.3799±0.01	0.3434±0.01	0.3271±0.01	0.3136±0.00	0.3659±0.02
0.6	0.4566±0.01	0.3981±0.01	0.3500±0.02	0.3164±0.01	0.2681±0.00	0.2571±0.00	0.2999±0.01
0.8	0.3704±0.00	0.3230±0.01	0.2839±0.01	0.2566±0.00	0.2444±0.00	0.2344±0.01	0.2734±0.01
1	0.3435±0.01	0.2996±0.01	0.2633±0.01	0.2380±0.00	0.2267±0.01	0.2174±0.02	0.2536±0.01
1.2	0.3435±0.00	0.2995±0.05	0.2633±0.00	0.2380±0.01	0.2267±0.00	0.2174±0.01	0.2536±0.00

Surrogate Modelling

A surrogate model is any model that mimics the relationship that the computational model establishes between the input variables and the quantity of interest (QoI). The significance of using a surrogate model in the propagation of uncertainties is to gain computation time. Many types of surrogate model have been proposed, the polynomial surrogate models are most often encountered. Over the last decade, attempts have been made to build surrogate models of deterministic functions. The most popular are Gaussian process modelling [28], generalized polynomial chaos expansion [29] and low rank tensor approximations [30].

Gaussian process (GP) regression, sometimes known as GP, is a popular approach for developing surrogate models with uncertainty quantification. This method has gained popularity in computer experiments [30] and now allows for scaling up in the number of learning points, thanks to the emergence of multi-fidelity codes, which has motivated the introduction of new GP regression approaches such as the Gaussian process auto-regressive or AR(1) scheme and the Deep GP method [31]. However, the existing autoregressive models and Deep GP can only be used for low-dimensional outputs.

In the case of polynomial chaos expansions (PCE) [32] the random fields of interest are approximated by expanding them in truncated series of random so-called polynomial chaos. Inserting these expansions into the original model yields the governing equations, which identify the unknown deterministic expansion coefficients. Since the governing equations are not the same as the model equation, the PCE technique is invasive. Thus, for models with limited accessibility, PCE may not be applicable. Stratified sampling techniques, such as Latin hypercube sampling (LHS), are used to improve the generation of random samples to allow for smaller sets giving rise to a higher computational efficiency.

On the other hand, if the random quantity is anticipated or expected, to exhibit a certain degree of smoothness along the stochastic space, a suitable and popular choice is to take advantage of the smoothness using a tensor approximation that rely on polynomials. Early efforts in this direction were reported to have used a univariate Hermite polynomials of zero-cantered, unit variance, normal random variables. So, tensorization of univariate Hermite polynomials leads to an orthogonal basis.

In this study, a Response Surface Methodology (RSM) and statistical sampling were deployed for building an approximation model. Collocation points were acquired experimentally using a 3-level factorial design in the Design Expert software version 11. The 32 experimental realizations of the IE obtained at different inhibitor concentrations (0.5-1.0

g/L); temperatures (30 - 60 °C) and immersion time (4-12 h) are presented in Table 2**.** The "+1", "−1," and "0" in the Table 2 denote the absolute high, low, and medium values of the corrosion factors, respectively. Apart from time-saving and minimum cost, from a few numbers of experimental runs, one can maximize information and develop efficient uncertainty RSM approximation model for uncertainty propagation.

A typical generalized polynomial model of second order can be constructed by finding the least-square fit between the responses and training data. Eq. 8 represents a quadratic proxy.

$$y(x) = \hat{y}(x) + \varepsilon, \quad x \in R^m \tag{8}$$

where ε represents the random error which is assumed to be normally distributed with a zero mean and a variance of σ^2. The error ε_i at any given observation is identically distributed since it is independent of other observations. To develop a correlation between x and y (see Eq. 9), the coefficients, β are carefully estimated such that the error is minimized.

$$\hat{y}(x) = \beta_0 + \sum_i \beta_i x_i + \sum_i \sum_j \beta_{ij} x_i x_j + \sum_i \beta_{ii} {x_i}^2 \tag{9}$$

where: x = vector of N input control parameters, β_i = coefficient of the linear model, β_{ij} = coefficient of interaction terms, and β_{ii} = coefficient of the 2nd order model.

Table 2. Responses of experimental design for inhibition process of mild steel in the presence of *Luffa Cylindrica* extract in 0.5M HCl [15]

Std	Run	Factor 1 X_1:inh.Conc g/l	Factor 2 X_2:Temp K	Factor 3 X_3:time h	Response 2 Inhibition efficiency %
4	1	0.50	318	4	76.92
18	2	1.00	333	8	87.38
13	3	0.50	318	8	77.42
15	4	1.00	318	8	83.09
2	5	0.75	303	4	71.73
28	6	0.75	318	8	79.64
3	7	1.00	303	4	73.64
10	8	0.50	303	8	70.77
21	9	1.00	303	12	75.68
22	10	0.50	318	12	78.74
11	11	0.75	303	8	73.27
14	12	0.75	318	8	79.64
7	13	0.50	333	4	84.38
19	14	0.50	303	12	71.55
27	15	1.00	333	12	87.98
16	16	0.50	333	8	85.42
30	17	0.75	318	8	79.64
9	18	1.00	333	4	86.81
1	19	0.50	303	4	69.80
31	20	0.75	318	8	79.64
32	21	0.75	318	8	79.64
6	22	1.00	318	4	82.39
29	23	0.75	318	8	79.64
23	24	0.75	318	12	80.72
17	25	0.75	333	8	86.81
5	26	0.75	318	4	79.73
25	27	0.50	333	12	85.73
8	28	0.75	333	4	85.21
24	29	1.00	318	12	84.06
26	30	0.75	333	12	87.34
12	31	1.00	303	8	74.34
20	32	0.75	303	12	74.32

The model uncertainty was first reduced by evaluating the linear, factorial (2F), quadratic, cubic and quartic models using sequential p-value, lack-of-fit, correlation coefficient and predicted correlated coefficient indicators using the analysis of variance technique [33]. The analysis revealed that the quadratic model is the most significant at 95% confidence level (α = 0.05) based on the F-value of 4100.49 and p-value <0,0001 recorded as shown on the ANOVA table presented in Table 3. From Table 3, it is observed that the large F-value obtained indicates non-significant noise and the p-value which is less than 0.05 suggests the model is significant. The model terms A, B, C, AB, BC, A^2, and B^2 show a high impact on the IE. The developed model for IE is given in Eq. 10.

$$IE\% = 3.67979 + 51.9421x_1 - 0.153920x_2 - 0.108889x_3 - 7.50642\,x_1^2 + 0.001132x_2^2 - 0.108889x_1x_2 - 0.003644x_2x_3 \quad (10)$$

where x_1, x_2 and x_3 represent Inhibition Concentration, Temperature and Time, respectively.

The Values of R^2, Adjusted R^2 and predicted R^2 of 0.9993, 0.9985 and 0.9991 indicate the developed model is excellent and predictable. The plot of the predicted IE against the experimental corrosion IE of the Luffa Extracts is shown in Fig. 2 which indicates about 99% of data points are along the $x = y$ line. This shows that the developed model exhibits a very high efficiency in predicting the experimental IE.

Table 3. ANOVA for Inhibition Efficiency for the Response Surface Model

Source	Sum of Squares	Df	Mean Square	F-value	p-value	
Model	845.39	7	120.77	4100.49	< 0.0001	Significant
x_1	30.49	1	30.49	1035.34	< 0.0001	
x_2	773.18	1	773.18	26251.74	< 0.0001	
x_3	10.09	1	10.09	342.66	< 0.0001	
x_1x_2	2.00	1	2.00	67.93	< 0.0001	
x_2x_3	0.5092	1	0.5092	17.29	0.0005	
x_1^2	1.13	1	1.13	38.48	< 0.0001	
x_2^2	0.3148	1	0.3148	10.69	0.0040	
Residual	0.5596	19	0.0295			
Lack of fit	0.5596	14	0.0400			
Pure Error	0.0000	5	0.0000			
Cor Total	845.95	26				
Std. Dev.	0.1716					
Adeq Precision	197.0976					

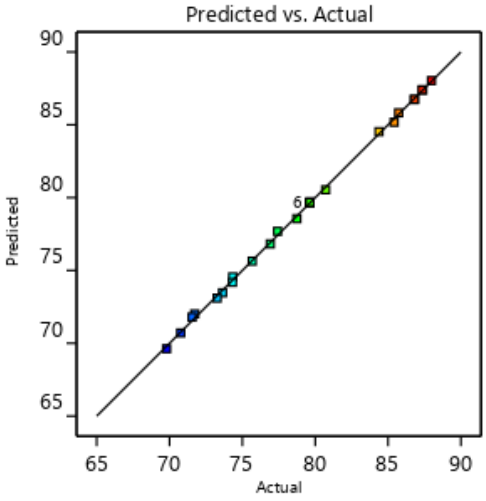

Fig. 2. Parity Plot of proxy predicted vs actual IE

Uncertainty Quantification Methods

Uncertainty quantification method can be deterministic or stochastic [34]. In the deterministic method, output uncertainty is expressed as a function of input uncertainties using Taylor series expansion, Hermite polynomials or basis functions [34]. Some examples of such method are generalized Polynomial Chaos (gPC), Gaussian closure, Equivalent linearization and the use of meta-models [30]. Deterministic methods are more suited for linear problems and in cases where uncertainties are relatively small. On the other hand, stochastic methods include Monte-Carlo (MC), Latin Hypercube Sampling (LHS) and Fourier Amplitude Sensitivity Test (FAST). Stochastic methods are computational cost. Nevertheless, they are widely used in various fields of science and engineering.

Many frameworks such as those that based on fuzzy-set theory, interval theory, evidence theory, and probability theory have been investigated for uncertainty quantification. These frameworks considered limitations inherent in experimental, modelling, and computation. Of all these frameworks, the probability theory is most popular because it has proved to facilitates a unified treatment of parametric uncertainties and modelling errors. In uncertainty quantification, we seek to establish theory, methods, and computer programs for effective management of the ensuing parametric uncertainties, modelling errors, and computational errors in predictive simulations. The three important processes are: characterization, propagation, and sensitivity analysis.

The process of incorporating uncertainty to computational models is termed characterization. The common approaches include parametric, nonparametric, output-prediction-error approaches, and generalized or hybrid approaches that couple parametric and nonparametric approaches [30]. Parametric approaches involve the characterization of some or all parameters as random variables, stochastic processes, or both. On the other hand, when the uncertain features of the computational model cannot be associated with uncertainties in some or all of the parameters, nonparametric approaches are adequate. The output-prediction-error approaches involves the addition of a random noise term to the quantity of interest.

To propagate uncertainty, the probability theory equates the probability of QoI with the probability that the value taken by the uncertain input variables is contained in the corresponding subset. This is most often implemented using either the Monte Carlo sampling method or stochastic expansion methods which required fitting surrogate model to the computational model; then, the characterization of the uncertain input variables is mapped through this surrogate model into the characterization of the quantity of interest [35].

The objective of the sensitivity analysis is to gain some insight into the manner in which uncertainties introduced in the input variables induce that in the QoI. Such insight can be very useful for identifying where to direct efforts aimed at reducing uncertainties, and it can constitute a crucial prerequisite to the optimization of designs in the presence of uncertainties and the validation of models, among other purposes. Several types of sensitivity analysis of uncertainties can be used and have been proposed in the literature, such as methods involving scatter plots and regression, correlation, and elementary effects, methods involving variance analysis, and methods involving differentiation [36].

Optimization with Uncertainty Consideration

Two methods were investigated in this study for performing the optimization and uncertainty quantification. The first method is the Monte-Carlo Simulation (MCS) method, which is the most common robust optimisation method to find the probability distribution of an objective function that has been predefined to include uncertainties. This method involves the use of an

approximation model to reduce computational costs. Unfortunately, unless the surrogate model perfectly mimics the computational model, the use of the surrogate model introduces an approximation error in the characterization of the QoI. Also, the variables included in the optimisation routines to account for uncertainty are often limited so, significant uncertainties can be neglected. Thus, the optimisation results were not always "true" and may be overly optimistic. In general, the challenges with optimization under uncertainties is the determination of number of model realisations to adequately capture and represent the true distribution of uncertainty at a minimum computation cost.

By performing optimisation on a selected number of models out of large set of models can be beneficial in terms of computation time and cost. Efforts in this regard include the use of techniques such as k-means clustering and non-dominated sorting algorithm to help in selecting the "best" solutions for nominal optimisation and optimisation under uncertainty [37]. However, an attempt to reduce the complexity of the optimisation problem by ranking realisations has been made which has limited the optimisation to a few realisations and the actual distribution of uncertainties is neglected. To address some of the challenges enumerated we applied Markowitz classical optimisation theory, to the mean-variance objective function and robust optimisation was performed under uncertainty using the Genetic Algorithm (GA). The mean-variance function is similar to a double objective problem which is transformed to single-objective optimisation using the weighting function, λ.

Regular Monte Carlo Simulation

The characterization, propagation and sensitivity analysis were carried out using the Oracle Crystal Ball Fusion Edition v11.1.1.1.00. The key activities include (i) defining decision variable IE, and assigning the distribution functions to process parameters (ii) propagate the uncertainties using RSM approximation model, and (iii) performing sensitivity analysis. A 2-parameter uniform distribution function was assumed since the probability density function is expected to be constant within the interval ($a < X < b$) and zero outside that interval. This allows for sampling within the specified limit of various parameters which are concentration (0.5-1.0 g/L), temperature (303-333 K), and time (4-12 h) using a MC sampling technique. To allow for a wide range of coverage, 10,000 trials of random numbers was assumed for the simulation. After the simulation trials were completed, the output results were analysed and realizations were ranked using P10-P90. The realization with a rank of P10 indicates that the recorded value of IE has a 10 percent chance of occurrence. While the P90 indicates 90 percent chances of occurrence. The wider the difference between these probabilities, the more uncertain is the QoI.

Mean -variance method

One well-known method for carrying out optimization under uncertainty in financial operations is the Markovitz classical theory [37]. Many studies have adopted this technique which involves estimation of the efficient frontier otherwise known as mean-variance to reflect how the reward varies with uncertainties. In the context of corrosion inhibition optimization, the reward is the predicted IE which in this study is uncertain. The uncertainty is computed using the variance of the IE. To demonstrate this technique, the process response (f) was modelled as shown in Eq. 11:

$$f = f(\alpha) \tag{11}$$

where, $\alpha = \{\alpha 1, \alpha 2, \alpha 3, \ldots, \alpha_N\}$ are set of unknown variables that affect the corrosion inhibition process. If in a model with m unknown parameters, n points are utilized to describe the distribution of an uncertain parameter, $N = m^n$ realisation of uncertainty will be needed to sufficiently sample the uncertainty space. The mean and standard deviation for N realizations is provided in Eq. 12 and 13, respectively.

$$\mu(\alpha) = \frac{1}{N}\sum_{i=1}^{N} f_i(\alpha) \quad (12)$$

$$\sigma(\alpha) = \sqrt{\frac{1}{N}\sum_{i=1}^{N}(f_i(\alpha) - \mu(\alpha))^2} \quad (13)$$

The procedure for this method is summarized as follows:

Step 1. Generate n=100 random number of concentration (0.5-1.0 g/L), temperature (303-333 K), and time (4-12 h) using MC random generator.

Step 2. Construct n=100 IE realization model using approximated model

Step 3. Calculate $F_\lambda = \mu(\underline{\alpha}) - \lambda\sigma(\underline{\alpha})$ for a chosen ʎ.

where the risk-aversion factor, denoted by λ determines the degree of uncertainty tolerance. A higher λ value denotes a lower risk preference and a stronger aversion to risk, which might lead to a better degree of decision-making confidence. In the case of normally distributed samples, λ values of 0, 1, 2, 3 and 4 correspond to 50.00, 84.13, 97.72 and 99.99% confidence [38]. These five confidence levels are chosen for the optimisation method to allow for a wide range of risk tolerance [39].

Step 4. Perform optimization using GA

During the optimization phase, a search algorithm is employed to determine the maximum value of F for a particular model realization. The procedure is then repeated for various values of λ. On the mean-variance plot, all models can be plotted, but the optimal cases for each typically lie on the efficient frontier, though other models may as well.
To optimize the IE using a mean-variance approach, the objective function is defined as follows:

$$F_\lambda = \mu(\underline{\alpha}) - \lambda\sigma(\underline{\alpha}) \quad (14)$$

In this study, the implementation of the GA with MATLAB, (2019) was carried out to obtain the optimal solution of IE of *Luffa Cylindrica extract*. The best fitness value was attained after the 25th generation after setting each generation at a population of 100 and a chance of mutation of 5% according to [37]. To ensure a global optimum solution, the experiments were repeated thrice. Fig. 3 shows the GA workflow algorithm used in this study which includes population generation, evaluation, reproduction, elitism, crossover, and mutation [40].

Step 5. For optimal F, plot $\mu(\alpha)$ against $\sigma(\alpha)$, and identify the efficient frontier.

From a set of *N* individual realisations of *f* sampled using different values of α, the mean-variance plot can be constructed by plotting $\mu(\alpha)$ against $\sigma(\alpha)$. The efficient frontier is then determined by selecting points that have a higher μ than any other point with the same σ. Following that, Markowitz maximizes μ for a specified σ and minimizes σ for a specified μ.

Step 6. Rank the solution using non-dominated sorting technique

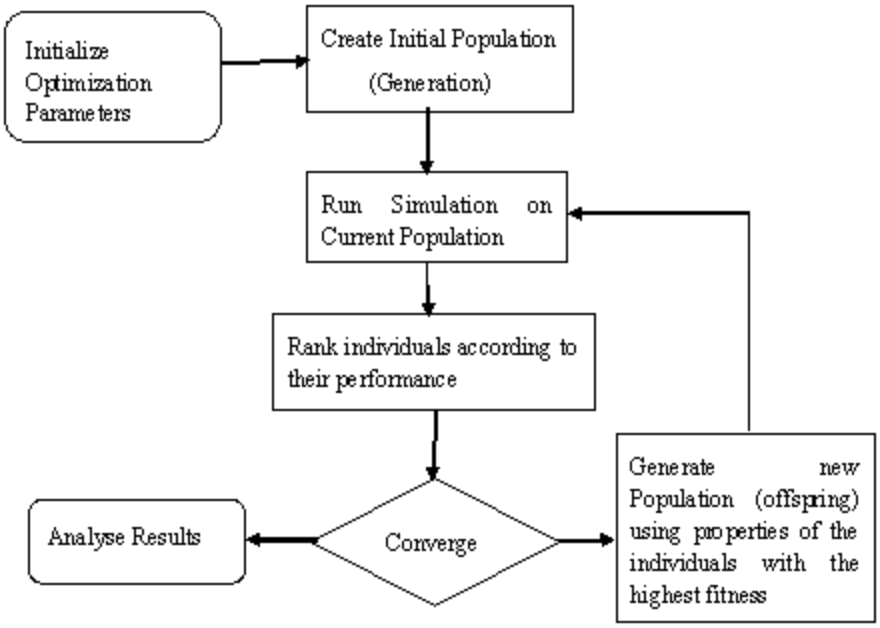

Fig. 3. Workflow of the Genetic Algorithm methodology

Results and Discussions

Batch Corrosion Study

The result of the weight loss (Table 1) revealed a significant reduction in the material loss with an increase in extract concentration which decreases with time. Comparing this observation with the control solution shows clearly that the corrosion of mild steel in 0.5 M HCl solution was inhibited in the presence of the *Luffa Cylindrica* extract molecules by adsorbing on the mild steel surfaces thereby forming a thin film that prevented direct contact of the acid and mild steel [15, 41]. The inhibition efficiency (Fig. 4) however was observed to increase with the extract concentrations until equilibrium was attained at 1.0 g/L after 144 h which resulted in an IE of 82.47%. Green inhibitors generally are highly sensitive to temperature [1, 15, 17]. For practical applications in the chemical and related industries, investigation of the thermal stability of green inhibitors at temperatures other than the ambient is critical. However, previous studies have shown that many plant extracts are thermally stable at temperatures between 30-60 C [6], [15, 22].

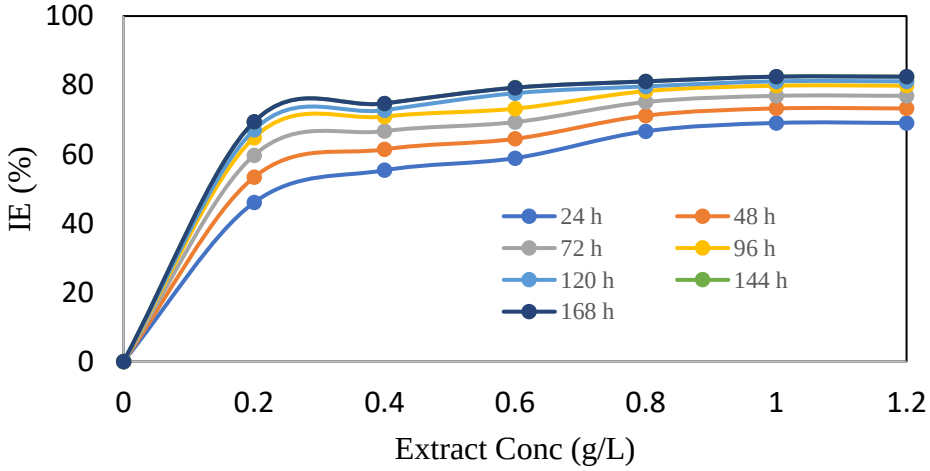

Fig. 4. Extract's corrosion inhibition efficiency in the absence and presence of different concentrations of *Luff cylindrical* extract at room temperature (30±0.5°C)

Effects of Factors on IE

The plot showing the effects of inhibition concentration, temperature and immersion time is shown in Fig. 5. Fig. 5a is a sensitivity plot which compares the effects of the corrosion factors at base value (0) in the design space. The IE was estimated and plotted by changing only one factor, say temperature, over its range (303-333 K) while holding all the other factors constant. The steepest slope in the temperature trend (Fig. 5b) shows that the IE is most sensitive to temperature compared to other factors. The plot therefore showed that temperature (x_2) is a "heavy hitter" in this study and plays a dominant role in the designing of a *Luffa Cylindrical*-based inhibitor for the corrosion of mild steel. The displacement of the cube in the sensitivity plot towards the right-hand side shows high thermal stability and positive influence on IE while the marginal displacement observed in the case of inhibition concentration (x_1) and the immersion time (x_3) as is observed in Fig. 5c and 5d indicates a better understanding of these parameters from the preliminary study and therefore constitute a marginal level of uncertainty in the evaluation process.

Fig. 6 presents the 3D plots and contour maps that show the extent to which corrosion parameters interaction influences the IE. A strong synergy was observed among these factors and their interactions were observed to have a great influence on IE. However, temperature and inhibition concentration exhibit pronounced effects on the IE.

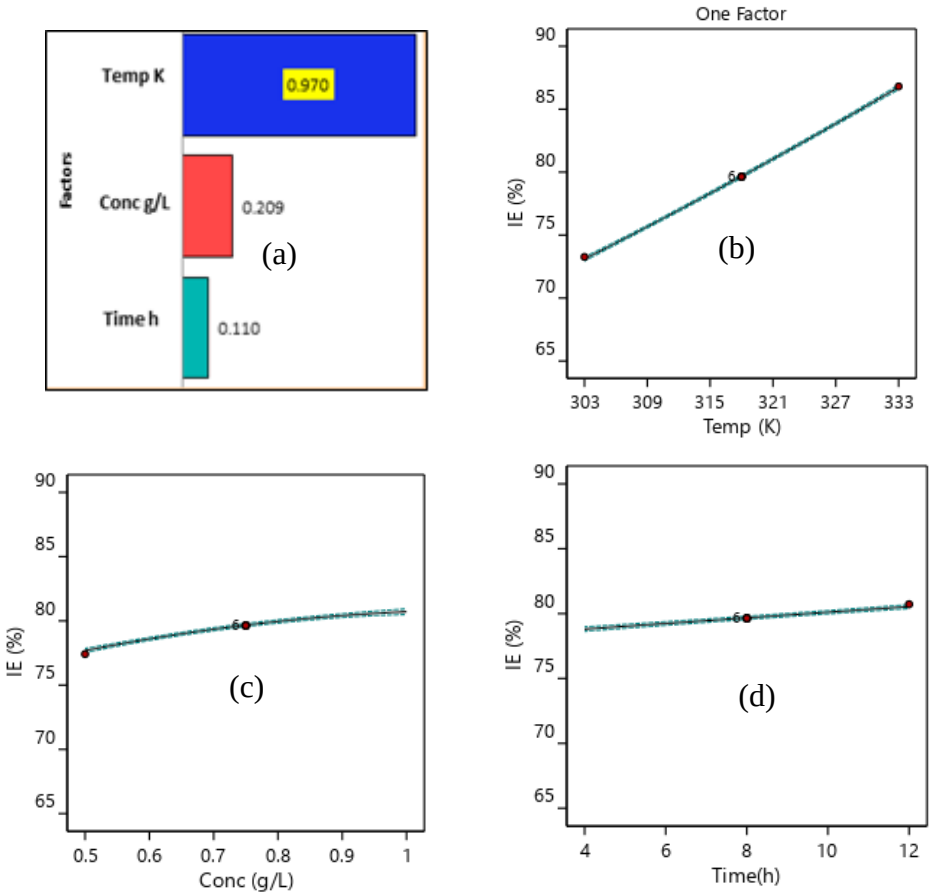

Fig. 5. Graph showing (a) Sensitivity plot (b) effect of temperature on IE (c) effect of Concentration on IE (d) effect of time on IE

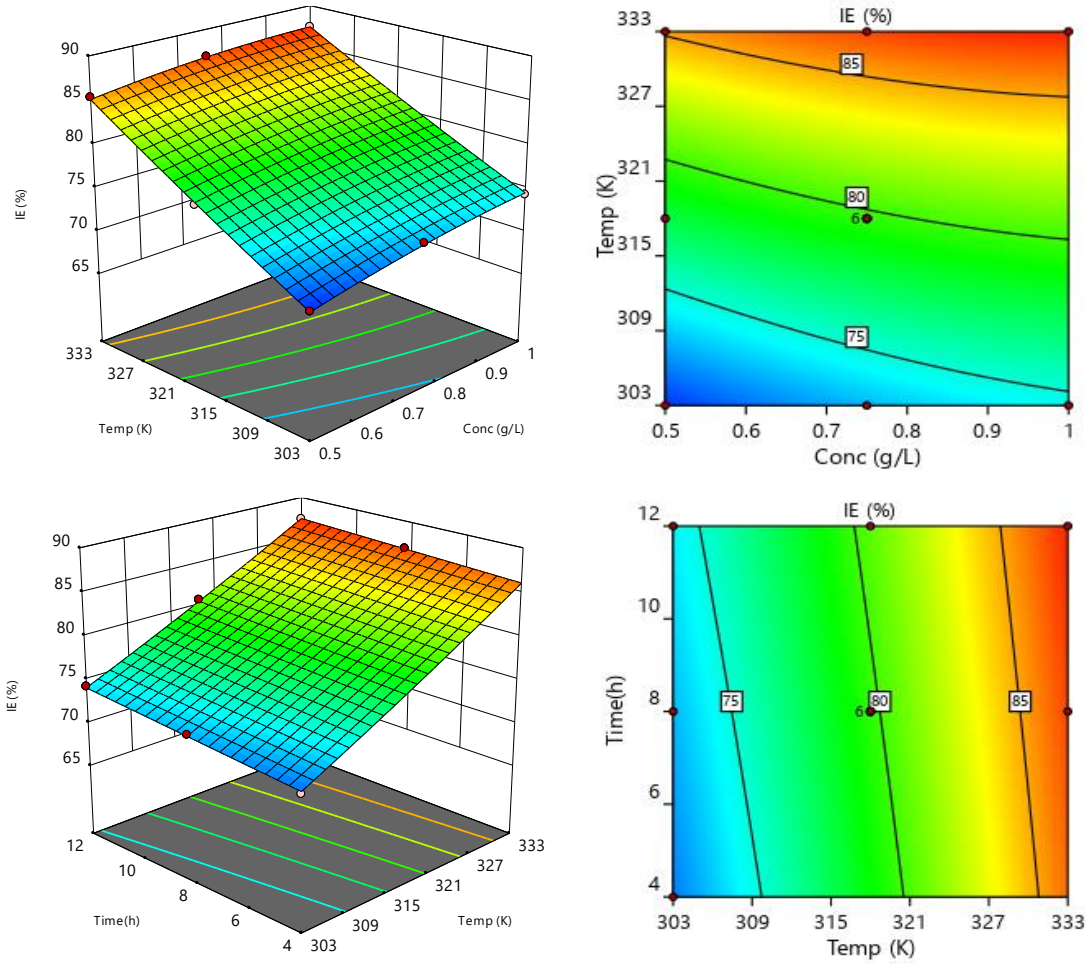

Fig. 6. 3D and Contour plots indicating the synergistic effects of (a) temperature and concentration and (b) Temperature and immersion time

Regular Monte Carlo Simulation

Fig. 7 shows the forecast chart for the Cumulative probability distribution of the Inhibition Efficiency which was best fitted to the beta-distribution function after 10,000 iterations (a and b respectively). Ten thousand iteratively built equiprobable realizations in Excel were found to be sufficient to stabilize the resulting forecast distributions. From the scatter plot shown in Fig. 8, it is obvious the correlation coefficient of temperature (x_2), Concentration (x_1), and Time (x_3) are 0.970, 0.209, and 0.113, respectively which indicates that temperature has the greatest influence on Inhibition Efficiency, followed by Concentration, and then Time. Table 4 shows the statistical analysis at the end of the forecast for IE after 10,000 iterations. The corresponding IE values obtained from the beta distribution are also displayed. The base case is 79.70 per cent at a mean standard error of 0.04 after the experimental validation which attests to the reliability of the simulation result. The P10 indicates 90% confidence with only 10% uncertainty while P100 indicates 0% confidence with 100% uncertainty. The P10, P20, P30, P40, P50, P60, P70, P80, P90, P100 is 74.14, 75.49, 76.74, 78.11, 79.48, 80.86, 82.27, 83.72, 85.16, and 87.9%, respectively. Therefore, the reported IE for *Luffa Cylindrica* of 88.4% [15] only deviated marginally from the P100 value of 87.8% reported in this study which makes the value highly optimistic.

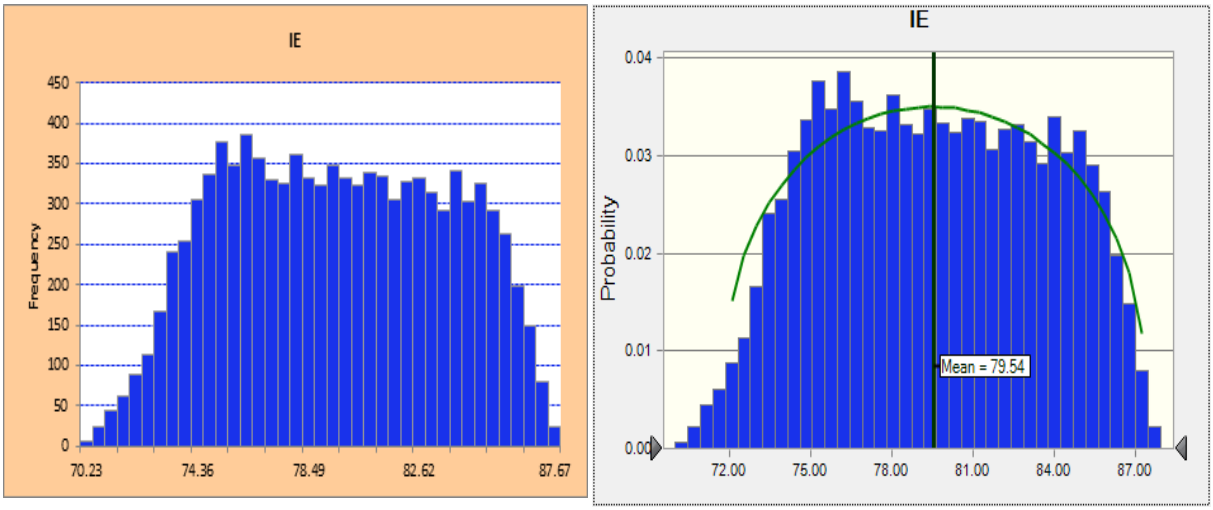

Fig. 7. (a) Cumulative Probability Distribution (b) Beta- Distribution

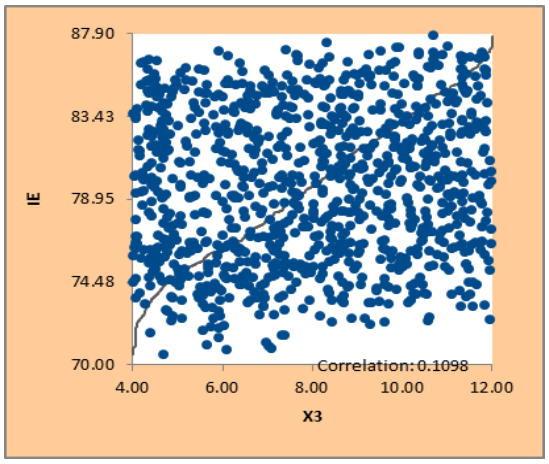

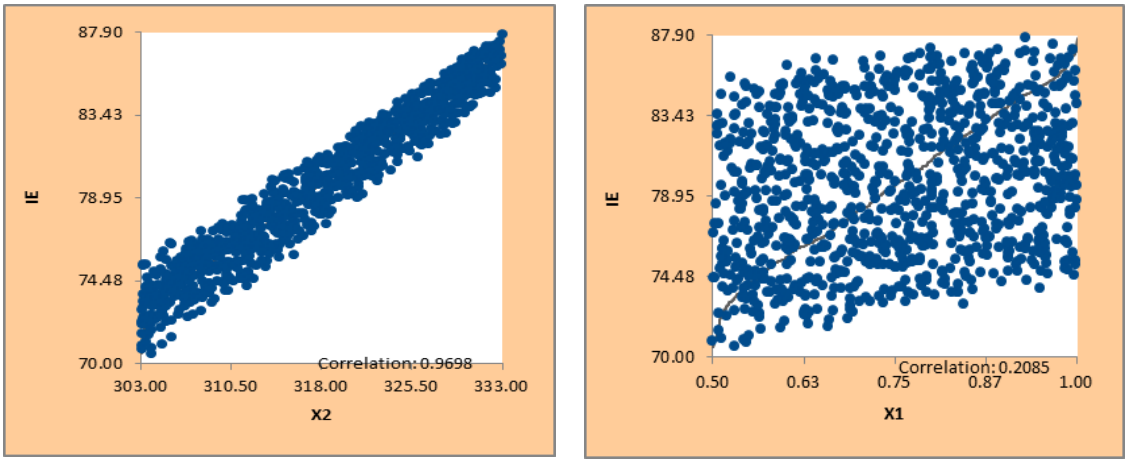

Fig. 8. Pareto Chart for Sensitivity analysis for the Forecast of IE and corresponding correlation of factor

Table 4. Statistical Analysis at the end of forecast IE and Beta-distribution function

Statistics	Fit-Beta	Forecast Values
Trials	-	10,000
Base Case	-	79.7
Mean	79.54	79.54
Median	79.53	79.48
Mode	79.48	---
Standard Deviation	4.08	4.09
Variance	16.73	16.73
Skewness	0.0039	0.0039
Kurtosis	1.96	1.95
Coeff. of Variation	0.0514	0.0514
Minimum	71.64	70
Maximum	87.47	87.9
Range Width		17.9
Mean Std. Error		0.04

Mean-Variance Method

Fig. 9 is the plot of mean values, $\mu(\underline{\alpha})$ of the IE against the standard deviation, $\sigma(\underline{\alpha})$ for different aversion factors λ =0, 1, 2, 3, 4. Each point on the graphs corresponds to $\mu(\underline{\alpha})$ and $\sigma(\underline{\alpha})$ of 100 each of the ensembles of the uncertainties. The mean fitness value after 25 iterations is the arithmetic average of the 100 objective functions of each generation. For each iteration, the standard deviation of the fitness value reduces, an indication that the simulation coverages reduce as the number of generations increases. The best and mean fitness values recorded are 79.132 and 79.1601%, respectively. The optimal IE obtained which correspond to 50.00, 84.13, 97.72 and 99.99% probability, is 79.7, 78.0279, 77.0279 and 76.5%, respectively.

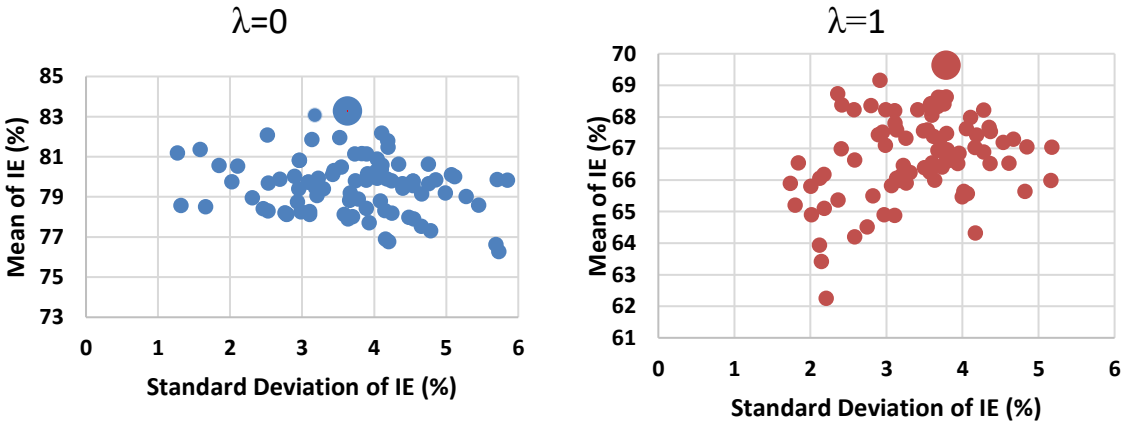

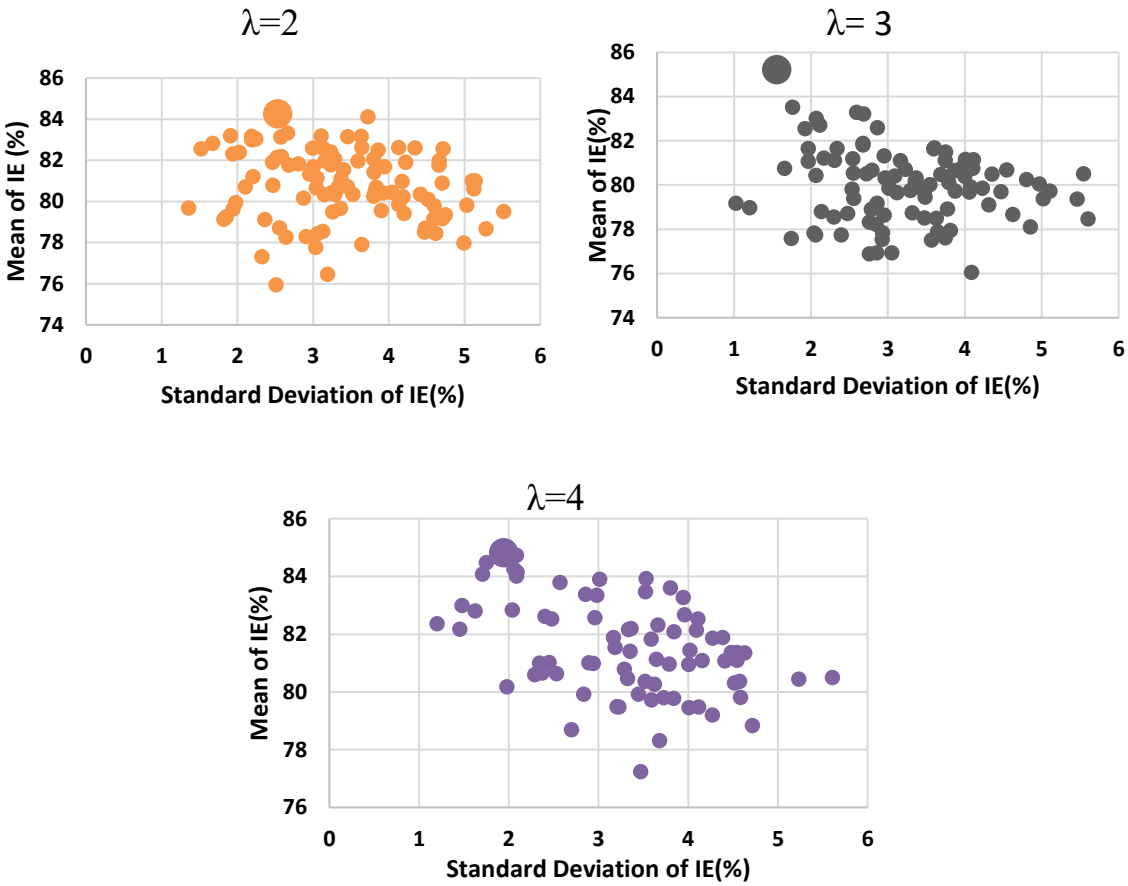

Fig. 9. Typical efficient frontier plot for different risk factors λ=0,1,2,3,4

Conclusion

Numerous factors do influence the corrosion process and many studies in the public domain seldom consider many of these factors which makes the outcome highly uncertain for practical and field applications. Green inhibitors are fast becoming the acceptable alternative for mitigating the corrosion of metals in acidic and other harsh media owing to environmental friendliness and availability. Several authors have evaluated different plant extracts and have reported inhibition efficiencies in the range between 80-97% [15]. The IE of *Luffa Cylindrica* leaf extract is quantified in this study using two distinct approximation models for uncertainty propagation. The following conclusions were drawn from this study:

i. The Markovich method shows at least 50% and 99.9% probabilities that the IE of *Luffa Cylindrica* leaf extract is 79.7% and 76.5%, respectively.
ii. The regular Monte Carlo Simulation indicates at least 10 and 90% probabilities that the IE of *Luffa Cylindrica* leaf extract is 85.16 and 74.14%, respectively.
iii. Both results indicate the reported IE for *Luffa Cylindrica* leaf extract is highly optimistic and uncertain judging from the outcome of this present study.
iv. Both methods agreed that the IE of 88.4% reported by [15] correspond to less than P50.
v. Therefore, the development of lifetime field-applicable green inhibitors must consider uncertainty quantification for more realistic decision-making.

Nomenclature

Symbol	*Definition*
β_a, β_c	Anodic and cathodic Tafel's slope
"i", "f" and "c"	Initial, final and cleaning
V_{unc}	variance of the uncertainty
δ_m	Standard deviation in the measurement of mass
δ_t	Standard deviation in the measurement of time
δ_A	Standard deviation in the measurement of area
ρ	Density
A	Surface area
t_o and t_f	Initial and final times
W_i, W_f	Initial weight, and final weight
α = {α1, α2, α3, …, α_N}	Set of unknown variables that affect the corrosion
λ	Risk-aversion factor
μ	Mean
σ	Variance
CR	Corrosion rate
IE	Inhibition Efficiency
QoI	Quantity of Interest

References

[1] Malaret F. Exact calculation of corrosion rates by the weight-loss method. Experimental Results. 2022; 3:1-12. doi: 10.1017/exp.2022.5.

[2] Autolab M. Application Area: Corrosion Electrochemical Corrosion Studies of Various Metals. Corrosion. 2018;1-11.

[3] Rybalka KV, Beketaeva LA, Davydov AD. Estimation of Corrosion Rate of AISI 1016 Steel by the Analysis of Polarization Curves and Using the Method of Measuring Ohmic Resistance. Russian Journal of Electrochemistry. 2021;57(1):16-21. doi: 10.1134/S1023193521010092.

[4] Verma DK, Dewangan Y, Dewangan AK, Asatker A. Heteroatom-Based Compounds as Sustainable Corrosion Inhibitors: An Overview. Journal of Bio- Tribo-Corrosion. 2021;7(1). doi: 10.1007/s40735-020-00447-7.

[5] Verma C, Ebenso EE, Quraishi MA, Hussain CM. Recent developments in sustainable corrosion inhibitors: Design, performance and industrial scale applications. Materials Advances. 2021;2(12):3806-3850. doi: 10.1039/d0ma00681e.

[6] Ogunleye OO, Eletta OA, Arinkoola AO, Agbede OO. Gravimetric and quantitative surface morphological studies of Mangifera indica peel extract as a corrosion inhibitor for mild steel in 1 M HCl solution. Asia-Pacific Journal of Chemical Engineering. 2018;13(6). doi: 10.1002/apj.2257.

[7] Alaiya MA, Odeniyi MA. Utilisation of Mangifera indica plant extracts and parts in antimicrobial formulations and as a pharmaceutical excipient: a review. Future Journal of Pharmaceutical Sciences. 2023;9(1). doi: 10.1186/s43094-023-00479-z.

[8] Barghout NA, El Nemr A, Abd-El-Nabey BA, Fetouh HA, Ragab S, Eddy NO. Use of orange peel extract as an inhibitor of stainless-steel corrosion during acid washing in a multistage flash desalination plant. Journal of Applied Electrochemistry. 2023;53(2):379-399. doi: 10.1007/s10800-022-01772-0.

[9] Umoren SA, Eduok UM, Solomon MM, Udoh AP. Corrosion inhibition by leaves and stem extracts of Sida acuta for mild steel in 1 M H2SO4 solutions investigated by chemical and spectroscopic techniques. Arabian Journal of Chemistry. 2016;9: S209-S224. doi: 10.1016/j.arabjc.2011.03.008.

[10] Omotioma M, Onukwuli OD. Evaluation of pawpaw leaves extract as anti-corrosion agent for aluminium in hydrochloric acid medium. Nigerian Journal of Technology. 2017;36(2):496. doi: 10.4314/njt. v36i2.24.

[11] Olawale O, Idefoh CK, Ogunsemi BT, Bello JO. Evaluation of groundnut leaves extract as corrosion inhibitor on mild steel in 1m sulphuric acid using response surface methodology (RSM). International Journal of Mechanical Engineering and Technology. 2018;9(11):829-841.

[12] Valdez-Salas B, Mirabal-García SF, Villalobos-Noriega JM, Lizardi-Jiménez MA, Hernández-Cocoletzi H, Zamudio-Flores PB, et al. Azadirachta indica leaf extract as green corrosion inhibitor for reinforced concrete structures: Corrosion effectiveness against commercial corrosion inhibitors and concrete integrity. Materials (Basel). 2021;14(12). doi: 10.3390/ma14123326.

[13] Loto CA, Loto RT, Popoola API. Effect of neem leaf (azadirachita indica) extract on the corrosion inhibition of mild steel in dilute acids. International Journal of Physical Sciences. 2011;6(9):2249-2257. doi: 10.5897/IJPS11.385.

[14] Soltani N, Khayatkashani M. Gundelia tournefortii as a green corrosion inhibitor for mild steel in HCl and H2SO4 solutions. International Journal of Electrochemical Science. 2015;10(1):46-62. doi: 10.1016/s1452-3981(23)04974-x.

[15] Ogunleye OO, Bamgbose JT, Odetoye TE, Olabisi AO. Green corrosion inhibition and adsorption characteristics of Luffa cylindrica leaf extract on mild steel in hydrochloric acid environment. Heliyon. 2020;6(1). doi: 10.1016/j.heliyon. 2020.e03205.

[16] Roseline UP. World Journal of Engineering DESIGN, EVALUATION AND PREDICTION OF CORROSION RATES. World Journal of Engineering Research and Technology. 2023;9(9):14-29.

[17] Zelinka SL. Uncertainties in corrosion rate measurements of fasteners exposed to treated wood at 100 % relative humidity. Journal of Testing and Evaluation. 2007;35(1):106-109. doi: 10.1520/jte100040.

[18] Freeman RA, Silverman DC. Error propagation in coupon immersion tests. Corrosion. 1992;48(6):463-466. doi: 10.5006/1.3315961.

[19] Rebak RB. Environmental Degradation of Engineered Barrier Materials in Nuclear Waste Repositories. Uhlig's Corrosion Handbook. Third Edition. 2011;503-516. doi: 10.1002/9780470872864.ch36.

[20] Fritz JD, Film Formation and CO2 Corrosion in the Presence of Acetic Acid. Thesis. 2004;1-97.

[21] Stansbury EE, Buchanan RA. Fundamentals of Electrochemical Corrosion. Ohio, USA: American Technical Publishers Ltd; 2000.

[22] Ogunleye OO, Eletta OA, Arinkoola AO, Bamgbose JT, Odetoye TE, Ayeni AO. Synthesis of green corrosion inhibitor for mild steel in acidic environment. Indian Chemical Engineer. 2020;62(1). doi: 10.1080/00194506.2019.1625815.

[23] Mahadevan S, Liang B. Error and Uncertainty Quantification and Sensitivity Analysis in Mechanics Computational Models. International Journal of Uncertainty Quantification. 2011;1(2):147-161. doi: 10.1615/intjuncertaintyquantification. v1.i2.30.

[24] Freeman RA. Error propagation and uncertainty analysis: Application to fault tree analysis. Process Safety Progress. 2020;39(2):1-12. doi: 10.1002/prs.12080.

[25] Agarry SE, Oghenejoboh KM, Aworanti OA, Arinkoola AO. Biocorrosion inhibition of mild steel in crude oil-water environment using extracts of Musa paradisiaca peels, Moringa oleifera leaves, and Carica papaya peels as biocidal-green inhibitors: kinetics and adsorption studies. Chemical Engineering Communications. 2019;206(1). doi: 10.1080/00986445.2018.1476855.

[26] Arinkoola AO, Onuh HM, Ogbe DO. Quantifying uncertainty in infill well placement using numerical simulation and experimental design: case study. Journal of Petroleum Exploration and Production Technology. 2016;6(2). doi: 10.1007/s13202-015-0180-z.

[27] Carmona VB, Oliveira RM, Silva WT, Mattoso LH, Marconcini JM. Nanosilica from rice husk: Extraction and characterization. Industrial Crops and Products. 2013;43(1). doi: 10.1016/j.indcrop.2012.06.050.

[28] Jiang Z, Apley DW, Chen W. Surrogate preposterior analyses for predicting and enhancing identifiability in model calibration. International Journal of Uncertainty Quantification. 2015;5(4):341-359. doi: 10.1615/Int.J.UncertaintyQuantification.2015012627.

[29] Yuen KV, Ortiz GA. Bayesian nonparametric general regression. International Journal of Uncertainty Quantification. 2016;6(3):195-213. doi: 10.1615/Int.J.UncertaintyQuantification.2016016055.

[30] Arnst M, Ponthot JP. An overview of nonintrusive characterization, propagation, and sensitivity analysis of uncertainties in computational mechanics. International Journal of Uncertainty Quantification. 2014;4(5):387-421. doi: 10.1615/Int.J.UncertaintyQuantification.2014006990.

[31] Kerleguer B, Cannamela C, Garnier J. A Bayesian neural network approach to multi-fidelity surrogate modelling. International Journal of Uncertainty Quantification. 2023;1-20. doi: 10.1615/Int.J.UncertaintyQuantification.2023044584.

[32] Mathelin L. Quantification of uncertainty from high-dimensional scattered data via polynomial approximation. Int. J. Uncertain. Quantif., vol. 4, no. 3, pp. 243–271, 2014, doi: 10.1615/Int.J.UncertaintyQuantification.2014008084.

[33] Arinkoola AO, Ogbe DO. Examination of experimental designs and response surface methods for uncertainty analysis of production forecast: A Niger Delta case study. Journal of Petroleum Engineering. 2015; 2015:1-16. doi: 10.1155/2015/714541.

[34] Wildey T, Gorodetsky AA, Belme AC, Shadid JN. Robust uncertainty quantification using response surface approximations of discontinuous functions. International Journal of Uncertainty Quantification. 2019;9(5):415-437. doi: 10.1615/Int.J.UncertaintyQuantification.2019026974.

[35] Hessling JP, Svensson T. Propagation of uncertainty by sampling on confidence boundaries. International Journal of Uncertainty Quantification. 2013;3(5):421-444. doi: 10.1615/int.j.uncertaintyquantification.2012004275.

[36] Gao X, Ying W, Zhang Z. An efficient numerical method for uncertainty quantification in cardiology models. International Journal of Uncertainty Quantification. 2019;9(3):275-294. doi: 10.1615/Int.J.UncertaintyQuantification.2019027857.

[37] Ogbeiwi P, Stephen KD, Arinkoola AO. Robust optimisation of water flooding using an experimental design-based surrogate model: A case study of a Niger-Delta oil reservoir. Journal of Petroleum Science and Engineering. 2020;195. doi: 10.1016/j.petrol.2020.107824.

[38] Ogbeiwi P, Stephen K, Arinkoola A. A surrogate-based approach to waterflood optimisation under uncertainty. In: ECMOR 2020 - 17th European Conference on the Mathematics of Oil Recovery. 2020. doi: 10.3997/2214-4609.202035076.

[39] Bailey WJ, Couët B, Wilkinson D. Field optimization tool for maximizing asset value. Proceedings of the SPE Asia Pacific Conference on Integrated Modelling for Asset Management. 2004;227-236. doi: 10.2118/87026-ms.

[40] Chen S, Li H, Yang D. Optimization of production performance in a CO2 flooding reservoir under uncertainty. Journal of Canadian Petroleum Technology. 2010;49(2):71-78. doi: 10.2118/133374-PA.

[41] Olusegun SJ, Alaneme KK, Olusegun SJ. Corrosion inhibition performance of lignin extract of sunflower (Tithonia diversifolia) on medium carbon low alloy steel immersed in H2SO4 solution. Leonardo Journal of Sciences. 2012;1-13. http://ljs.academicdirect.org/.

How to cite: Arinkoola AO, Oyelade EF, Omowumi AM, Gbolahan AA, Oluyemi AS, Ogunleye OO. Quantifying Uncertainty of Green Inhibition Efficiency of Luffa Cylindrica Leaf Extract on Mild Steel in Acidic Medium. Journal of Chemical and Petroleum Engineering 2024; 58(1): 189-207.